Supplementary Information

to the article

Bionanocomposite from self-assembled building blocks of nacre-like crystalline polymorph of chitosan with clay nanoplatelets

by Sergey Sarin, Sophia Kolesnikova, Irina Postnova, Chang-Sik Ha, Yury Shchipunov

1   Separation of chitosan crystalline polymorph

Chitosan macromolecules and saponite nanoparticles are associated one another through electrostatic interactions and hydrogen bonds. Smectite clays can be considered as polyelectrolytes in such mixtures.[1] As well-known (see, e. g. Refs. [2-4]), the maximal interactions occur at the stoichiometric ratio of oppositely charged constituents. It is reflected in the solubility of polyelectrolyte complexes that are insoluble in this vicinity in solvents of various polarity. It can be determined from the examination of swelling.

The water absorption by bionanocomposites was studied to find a region in which oppositely charged chitosan and saponite are close to their stoichiometric ratio. Owing to strong electrostatic interactions, bionanocomposites demonstrate the maximal stability.[5] A dried film weighted was placed in distilled water at 25˚C. Its weight was determined periodically after carefully removing of the H_2O excess from the surfaces. The swelling degree was calculated as:

$$\alpha = (m_s - m_d)/m_d \times 100\%,$$

where m_s и m_d are masses of swollen and dried film, respectively. Each experiment was repeated triply. Fig. 1S demonstrates how the swelling behavior in H_2O depends on the concentrations of chitosan and saponite in their mixtures. Areas of various film swelling are easily recognized by the color.
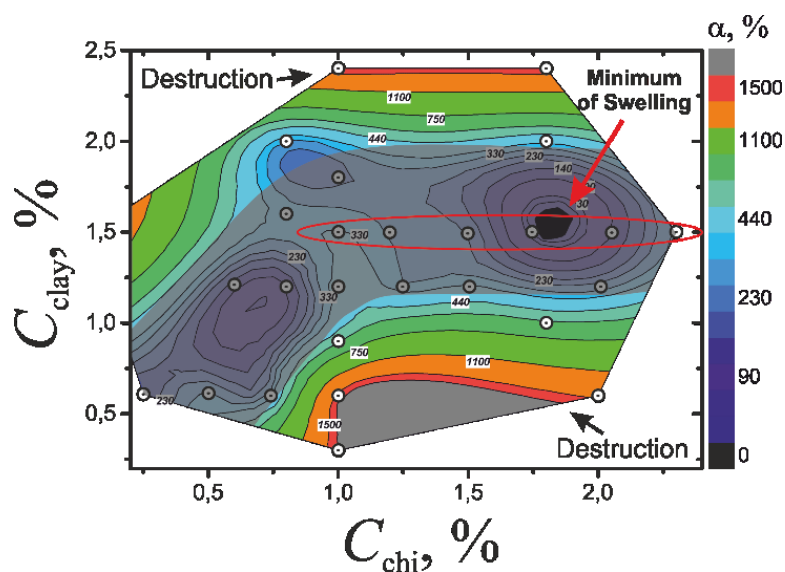

Figure 1S. The swelling degree of bionanocomposite films presented as chitosan vs. saponite concentrations in the forming solution. Difference in the α is obvious from the color of which the numerical value is shown in the right bar. White areas surrounding the color region correspond films undergoing a disintegration in the course of swelling.

The stability of chitosan polymorph in solvents is determined by the same electrostatic interactions and hydrogen bonds. To separate it from a film, the latter was placed in water. Its composition was a little far from the stoichiometric ratio of chitosan and saponite. In this case, films can absorb some amount of water, transferring into partially swollen state that facilitates the separation of crystalline polymorph. When it was made by treating them with the help of an ultrasonic dispenser, degraded pieces were found. They may be seen in Fig. 2S.
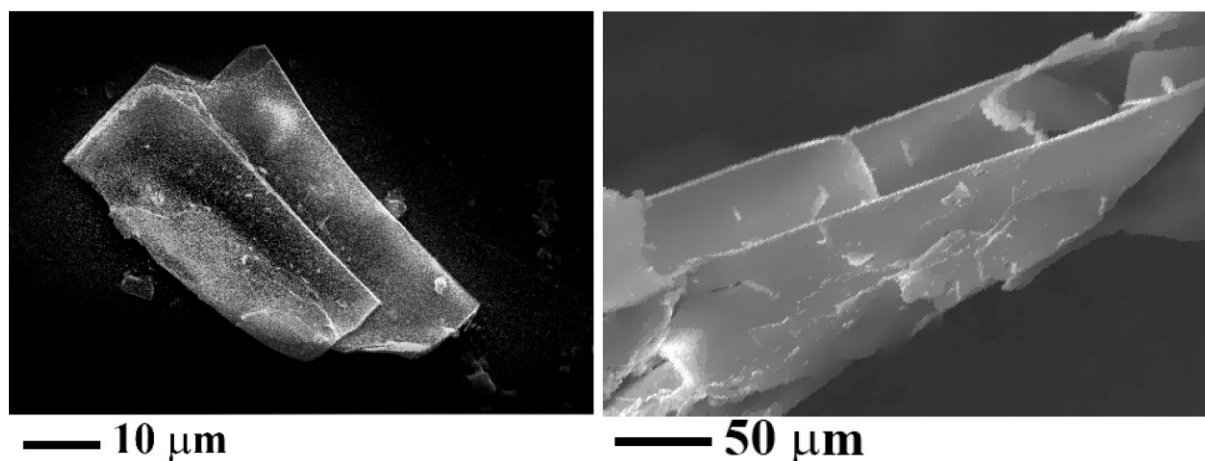

Figure 2S. SEM images of chitosan-saponite crystalline polymorph. Samples for the observation were prepared by placing a drop of highly diluted initial solution on a surface of freshly cleaved mica.

The interaction of chitosan with saponite nanoparticles was confirmed by using the microRaman spectroscopy. The spectra for chitosan, saponite and their bionanocomposite are presented in Fig. S3. Band assignment was done according to Ref. [6][1].
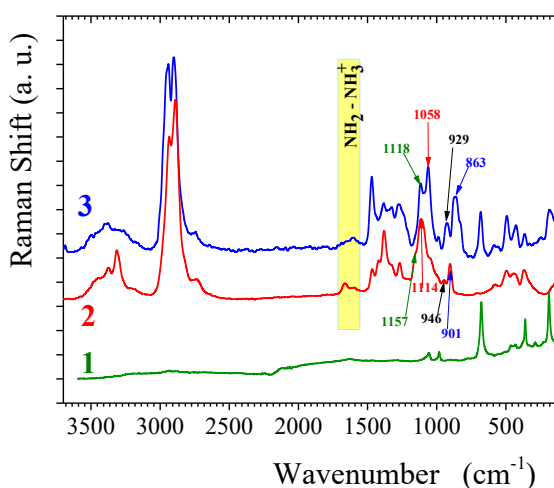

Figure 3S. Raman spectra of saponite (1), chitosan (2) and their bionanocomposite prepared at the stoichiometric ratio of polysaccharide and clay nanoparticles.

Amino group and their interactions with clay nanoparticles are usually identified through bands seen in the ranges 1580–1660 cm^{-1}(see, e. g., Refs. [7-10]). They characterize in-plane bending vibrations. One may find also them in the presenting spectra. There are notable changes in the band intensity and positon happened after chitosan mixing with saponite that may be related to the electrostatic interaction of protonated amine group with negatively charged sites on the clay surface.

Band at 946 cm^{-1} (curve 2) refers to the out-of plane vibrations of amino groups.[6] It offer a clearer recognizing the changes than previous ones. There are a significant increase of the band intensity and a shift of positon up to 929 cm^{-1} (curve 3). It provides further indication of interactions of amine group with clay nanoparticles in their bionanocomposite.

Pronounced changes are revealed in the in-plane stretching vibrations of pyranoid ring. It is obvious from the band at 901 cm^{-1} observed for chitosan (curve 2). Mixing with saponite resulted in a notable increase of intensity and shift it in a new position at 863 cm^{-1} (curve 3). Similar effect was observed in [11] in which chitosan salt with acetic acid were examined by means of Raman spectroscopy.

Further clear evidence of a decrease in mobility of pyranoid ring may be found from examination of bands characterizing C-O-C stretching vibrations at 1157 and 1114 cm^{-1} (curve 2).[6] There are also a substantial grow in their intensity and shift to 1118 and 1058 (curve 3). The decrease mobility of pyranoid ring points to a restricted motion of chitosan backbone that may be considered an additional confirmation of the polymorph formation.

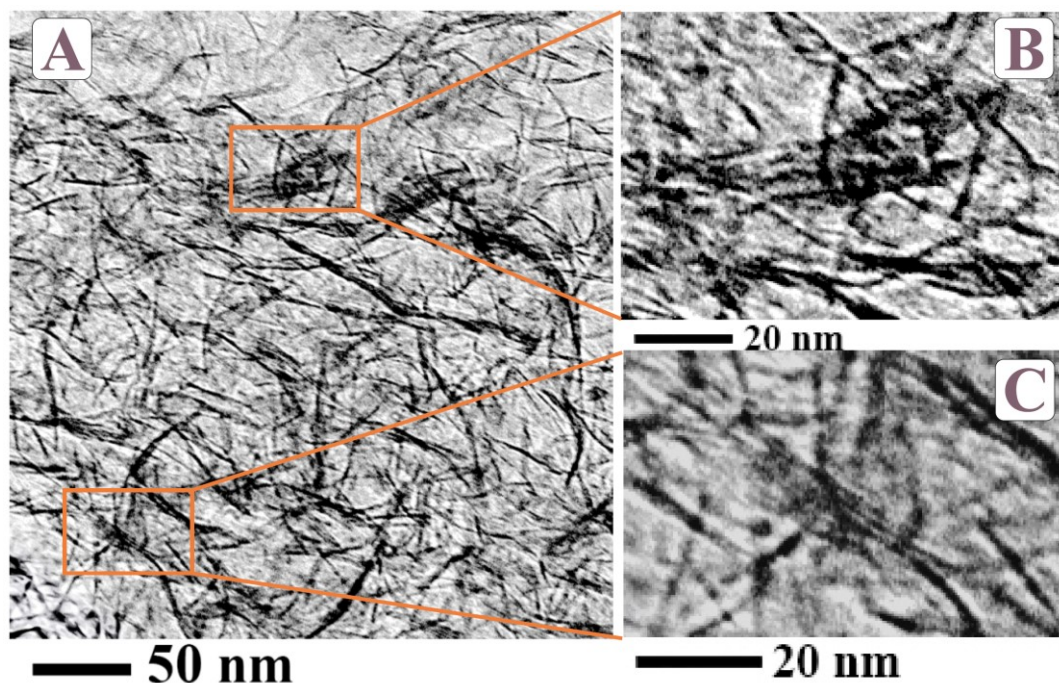## 2   Chitosan-saponite stacks visualized by TEM

Figure 4S. TEM images of chitosan-saponite stacks. General view of few stacks (A) and two of them at larger magnification (B, C) to see details. Repeating distance is equal to ca. 2 nm.

Sample was grinded, dispersed into acetone and then treated in the ultrasonic bath for an hour to have tiny pieces for examination. Few droplets of highly diluted dispersion were dripped onto a copper grid coated with an amorphous polymer or carbon film and dried under a warm air stream. There are still not-disintegrated chitosan-saponite stacks after this rather rigorous preparation.

3   Characterization of crystalline chitosan polymorph

There are as a whole 69 reflexes found in the diffractogram of chitosan-saponite bionanocomposite film presented in Fig. 2B (curve 3). 38 reflexes excluding minor ones are presented in Table 1S. Ogawa et al. determined 37 reflections for polymorph of this polysaccharide with hydriodic acid.[12] There is a good similarity for both the patters. Positions of 25 peaks agree very closely. There are also peaks differing in their position. Rows marked by green show reflections not mentioned by Ogawa et al., by yellow, not found in our diffractogram. Macromolecule conformation is very sensitive to surroundings. Exchange of iodide ion for clay nanoparticle should have a significant effect on the pattern. Peak shift is usually observed. It seems that it takes place in a case of reflexes 3, 6, 9 and 12 correlating with ones numbered 3a, 6a, 9a and 12a in the Table 1S. Peaks numbered 25, 26, 30-32, 34, 35 and 38 are very weak. They could not be well expressed in the diffractogram in the cited work. There is only a strong reflection missing in the publication of Ogawa et al. that is observed at $2\Theta = 5^{\circ}$ (numbered 1).

Rather good correlation of our WAXS data with results of Ogawa et al. allows us suggesting that crystalline polymorph of chitosan with saponite nanoplatelets has a similar conformation with that well characterized by Ogawa et al. in Ref. [12].

Diffraction reflexes presenting in the diffractogram of chitosan-saponite bionanocomposite film can be indexed by a tetragonal unit cell with dimension lattice parameters of $a \approx b \approx 10.7$ A and c (fiber axis) = 35.96 A from which only the c is highly accurate. This polymorph differs in the main from that described Ogawa et al. in the fiber period which was found by them to be 40.77 A.

Table 1S. WAXS data for polymorph of chitosan with saponite and hydriodic acid

№	$2\Theta^{a}$ (°)	$d_0{}^{b}$ (Å)	$d_{0 \text{ ref}}{}^{c}$ (Å)	Δ^{d} $\| d_0 - d_{0 \text{ ref}} \|$	hkl^{e}
1	5	17.5			
2	9.86	8.99	8.97	0,02	1 0 2
3	12.08	7.34			
3a			6.61		1 1 3
4	13.83	6.41	6.44	0,03	1 0 5
5	15.75	5.61	5.67	0,06	1 0 6
6a			5.54		1 1 5
6	16.35	5.43			
9a			5.27		2 0 0
7	17.29	5.14	5.10	0,04	1 0 7
8	17.85	4.97	4.97	0	1 1 6
9	18.46	4.82			
10	19.12	4.65	4.61	0,04	2 1 1
12a			4.52		1 0 8
11	20.04	4.43	4.46	0,03	2 1 3
12	20.92	4.26			
13	21.67	4.13	4.12	0,01	2 1 5
			4.17	0,04	1 0 9
			4.18	0,05	1 1 8

	2Θ[a]	d_0[b]	$d_{0\,ref}$[c]	Δ[d]	hkl[e]
14	22.32	3.98	3.89	0,09	2 1 6
15	23.63	3.77	3.81	0,04	1 1 10
	23.68	3.75		0,06	
16	24.69	3.61	3.68	0,07	3 1 0
			3.65	0,04	2 2 3
			3.64	0,03	2 1 8
17	25.24	3.54	3.52	0,02	1 0 11
18	26.75	3.34	3.31	0,03	2 1 9
			3.31	0,02	1 1 11
19	27.32	3.27	3.29	0,02	3 1 3
			3.29	0,02	3 1 5
20	29.29	3.05	3.03	0,02	3 0 8
21	29.79	3.00	3.01	0,01	3 2 0
22	30.56	2.93	2.99	0,06	1 0 13
23	31.4	2.85	2.88	0,03	1 1 13
24	31.85	2.82	2.82	0	3 1 8
25	32.33	2.77			
26	32.67	2.75			
27	33.01	2.72	2.72	0	2 0 14
28	33.8	2.65	2.65	0	3 3 0
			2.65	0	2 1 13
			2.65	0	2 1 15
29	34.51	2.60	2.60	0	3 1 11
30	35.33	2.54			
31	35.65	2.42			
32	37.6	2.39			
33	38.82	2.31	2.30	0,01	2 1 16
34	39.58	2.28			
35	40.37	2.23			
36	41.81	2.16	2.17	0,01	1 1 18
37	44.11	2.06	2.06	0	2 1 18
38	49.23	1.85			

[a] Values of angles 2Θ determined for chitosan-saponite film,

[b] d_0 spacing calculated from 2Θ,

[c] $d_{0\,ref}$ spacing for polymorph chitosan with hydriodic acid obtained in Ref. [12].

[d] Δ difference between d_0 and $d_{0\,ref}$,

[e] hkl miller indexes.

References

1   G. Lagaly, in *Developments in Ionic* Polymers, ed. A. D. Wilson and H. J. Prosser, Elsevier, London 1986, ch. 4, pp. 77-140.
2   A. B. Zezin and V. A. Kabanov, *Russ. Chem. Rev.* 1982, **51**, 1447.
3   E. Tsuchida and S. Takeoka, in *Macromolecualar Complexes in Chemistry and Biology*, ed. P. Dublin, J. Bock, R. Davis, D. N. Schulz and C. Thies, Springer, Berlin, 1994, ch. 12, pp. 183-213.
4   Y. A. Shchipunov and I. V. Postnova, *Composite Interf.* 2009, **16**, 251.
5   Y. A. Shchipunov, S. A. Sarin, V. E. Silant'ev and I. V. Postnova, *Colloid J.* 2012, **74**, 636.
6 1   G. Socrates, *Infrared and Raman characteristic group frequencies: Tables and charts*, Wiley, Chicheste, 2016.
7 2   M. Darder, P. Aranda, A. I. Ruiz, F. M. Fernandes and E. Ruiz-Hitzky, *Mat. Sci. Tech.*, 2008, **24**, 1100.
8 3   J. Kumirska, M. Czerwicka, Z. Kaczynski, A. Bychowska, K. Brzozowski, J. Thoeming and P. Stepnowski, *Marine Drugs*, 2010, **8**, 1567.
9 4   S. M. L. Silva, C. R. C. Braga, M. V. L. Fook, C. M. O. Raposo, L. H. Carvalho and E. L. Canedo, in *Infrared Spectroscopy - Materials Science, Engineering and Technology*, ed. T. Theophanides, InTech, Rijeka, Croatia, 2012, ch. 2, pp. 43-62.
10 5 J. B. Marroquin, K. Y. Rhee and S. J. Park, *Carbohyd. Polym.*, 2013, **92**, 1783.
11 6 G. Mikhailov, S. Tuchkov, V, V. Lazarev, V and E. Kulish, I, *Russ. J. Phys. Chem. A*, 2014, **88**, 936.

6   A. Lertworasirikul, K. Noguchi, K. Ogawa and K. Okuyama, *Carbohyd.Res.* 2004, **339**, 835.

References

1 G. Socrates, *Infrared and Raman characteristic group frequencies: Tables and charts*, Wiley, Chicheste, 2016.